VISUALIZATION OF THE NUCLEATION AND GROWTH OF PARTICLES

Darka Mioc ♭,
François Anton ♮,
Christopher M. Gold ♭♯

♭ Industrial Chair in Geomatics,
Centre de Recherche en Géomatique,
Université Laval,
Sainte-Foy, QC, G1K 7P4, Canada
E-mail: dmioc@cs.ubc.ca

♮ Department of Computer Science
University of British Columbia
201-2366 Main Mall,
Vancouver, B.C., V6T 1Z4, Canada
E-mail: fanton@cs.ubc.ca

♯ Department of Land Surveying and Geo-Informatics
Hong Kong Polytechnic University
Hung Hom, Kowloon, Hong Kong
E-mail: ChristopherGold@Voronoi.com

ABSTRACT

This article presents a method for the visualization of the nucleation and growth of particles based on an algorithm for the dynamic construction of additively weighted Voronoi diagrams. We use the Poisson point process in the dynamic additively Voronoi diagram to generate the Johnson-Mehl tesselation. The Johnson-Mehl model is a Poisson Voronoi growth model, in which nuclei are generated asynchronously using a Poisson point process, and grow at the same radial speed. Growth models produce spatial patterns as a result of simple growth processes and their visualization is important in many technological processes.

Keywords: Visualization of nucleation and growth of particles, Johnson-Mehl tessellations, Voronoi diagrams, growth models

1 INTRODUCTION

Particle statistics play an important role in many technological processes (in the industrial production of materials where the phase transition from liquid to solid is a part of the technological process, for example production of metals and ceramic materials) [Stoya98], material science, plant ecology, and spatial analysis.

Due to the lack of efficient algorithms for their visualization only the "set-theoretic approach in particle statistics" [Stoya98] has been used as a method of visualization of spatial growth processes.

Growth models produce spatial patterns as a result of simple growth processes operating with respect to a set of n points (nucleation sites), $\mathcal{P} = \{p_1, p_2, ...p_n\}$ at positions $x_1, x_2, ..., x_n$, respectively in $\mathbb{R}^m$ or a bounded region of $\mathbb{R}^m$ $(m = 2, 3)$. The growth processes such as agglomeration, aggregation, packing, etc. lead in a natural way to the Poisson Voronoi tessellation [Okabe92], [Stoya98] and to the Johnson-Mehl tessellation when the members of the generator set $\mathcal{P}$ are not contemporaneous [Okabe92].

The Johnson-Mehl model has been introduced in [Johns39] for modelling the growth of crystal aggregates. The Johnson-Mehl model is a Poisson Voronoi growth model, in which nuclei are generated asynchronously using a Poisson point process [Okabe92], and grow at the same radial speed v. Each generator $P_i = (\overrightarrow{p_i}, t_i)$ has both a planar location (its position vector) and an associated birth time t_i $(t_i \geq 0)$. The Johnson-Mehl tessellation can be considered equivalent to a dynamic version of an additively weighted Voronoi diagram [Anton98], in which the weight reflects the arrival time of the point in $\mathbb{R}^2$ [Okabe92]. The definition of the weighted Voronoi diagrams differs from the definition of the ordinary one in that the Euclidean distance is replaced by a weighted distance. In the case of the additively weighted Voronoi diagram, the weighted distance between a point and a generator is the Euclidean distance minus the weight of the generator. The additively weighted Voronoi diagram has been extensively studied by Ash and Bolker [Ash86] and Aurenhammer [Auren88] under the name of hyperbolic Dirichlet tessellations and Power Voronoi diagrams, but till [Mioc98] and [Anton98], there was no dynamic algorithm for constructing the additively weighted Voronoi diagram.

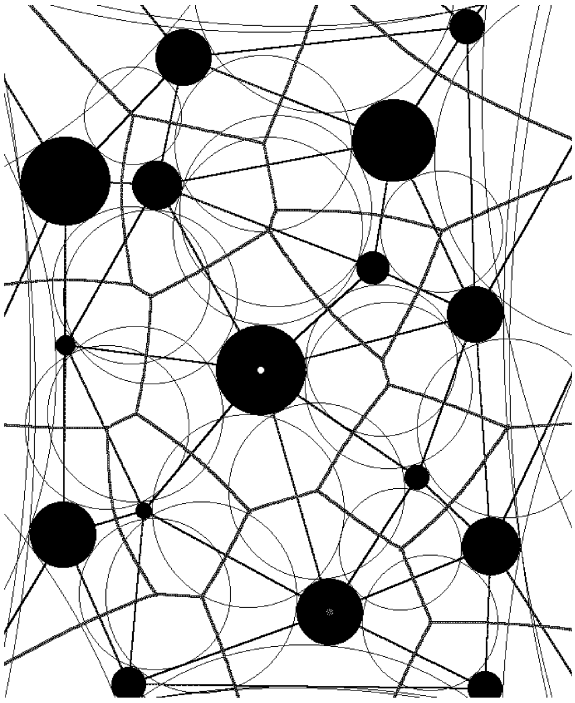

Figure 1: An additively Weighted Voronoi diagram.

In this paper, we introduce a new algorithm based on an algorithm for the dynamic construction of additively weighted Voronoi diagrams (see Figure 1, [Mioc98] and [Anton98]). We extend this algorithm to the incremental construction and visualization of nucleation and growth of particles using the Johnson-Mehl tessellation and the Voronoi growth model.

2 PRELIMINARIES

Let $\mathbb{R}^2$ be the Euclidean plane. Let $\mathcal{P} = \{P_i\}$ be the set of generators or nuclei, where $P_i = (\overrightarrow{p_i}, t_i)$ is defined by its position vector $\overrightarrow{p_i}$, and its birth time t_i. The nuclei are generated by a homogeneous Poisson point process [Horal79]. The cell $\mathcal{C}(P_i)$ generated by the growth of P_i contains all the points M such that the cell growing from P_i is the first one to meet M.

It is defined by: $\mathcal{C}(P_i) = \left\{ M \epsilon \mathbb{R}^2 \,/ \forall j : t_i + \frac{d(M,P_i)}{v} \leq t_j + \frac{d(M,P_j)}{v} \right\}$, where v is the constant radial growth of the nuclei. If we multiply both sides of the inequality inside the brackets by $v \geq 0$, and subtract vo where o is a constant, we get that $\mathcal{C}(P_i)$ is the set of points M of the plane such as $d(M,P_i) - v(o - t_i) \leq d(M,P_j) + v(o - t_j)$. By defining the weights of the nuclei as $w_i = v(o - t_i)$, we can see immediately the correspondence between the Johnson-Mehl tessellation and the additively weighted Voronoi diagram (shown on Figure 1) introduced in the previous section. The Johnson-Mehl tessellation for the set of points $\mathcal{P}$ is defined as $\mathcal{C}(\mathcal{P}) = \{\mathcal{C}(P_i) / P_i \in \mathcal{P}\}$. The cell $\mathcal{C}(P_i)$ is not empty if, and only if, for all j, $|v(t_j - t_i)| < d(M,P_j)$, that is to say the weight circle of P_i is not inside the weight circle of P_j.

We recall now a condition of the Johnson-Mehl model. If a point is born at a location that is already occupied by a growing cell, it disappears without trace [Okabe92]. We will suppose that we do not allow $|w_i - w_j| \geq d(P_i,P_j)$ for any P_i, and P_j of $\mathcal{P}$. This implies that no cell is empty in $\mathcal{C}(\mathcal{P})$, every vertex is 3-valent, and the Johnson-Mehl tessellation is proper, since the Johnson-Mehl tessellation can be considered equivalent to a dynamic version of an additively weighted Voronoi diagram [Anton98], [Okabe92], in which the weight reflects the arrival time of the point in $\mathbb{R}^2$. The additively weighted Voronoi region $\mathcal{V}(P_i)$ of P_i is the set of points M of the plane such as $\forall j : d(M,P_i) - w_i \leq d(M,P_j) - w_j$.

The additively weighted Voronoi diagram for the set of points $\mathcal{P}$ is defined as $\mathcal{V}(\mathcal{P}) = \{\mathcal{V}(P_i) / P_i \in \mathcal{P}\}$ (see Figure 1).

The bisector $\mathcal{B}_{ij}$ between P_i and P_j is the set of points M of the plane such as $\forall j : d(M,P_i) - w_i = d(M,P_j) - w_j$.

The valence of a vertex of a tessellation is the number of regions to which it belongs (from section 2 of [Ash86]).

A tessellation is proper if each region is regular, closed and at each vertex the angles formed by the tangent rays to the boundary curves which meet there are all less than π (see section 2 of [Ash86]).

Let $\mathcal{C}(P,w)$ be the weight circle of P, which is the circle whose centre is P and radius is w.

It is evident that $\mathcal{B}_{ij} = \mathcal{V}(P_i) \cap \mathcal{V}(P_j)$. We can express $\mathcal{B}_{ij}$ as the set of points M of the plane such as $\forall j : d(M,P_i) - d(M,P_j) = w_i - w_j$.

This locus is the branch of hyperbola whose foci are P_i and P_j, that is convex if $w_i \leq w_j$ (see Figure 1), and whose big axis is $a = \frac{w_i - w_j}{2}$.

The equation of such a hyperbola in polar coordinates is: $\rho = \frac{p}{1 - e\cos\theta}$ where e is the eccentricity of the hyperbola: $e = \frac{d(P_i,P_j)}{|w_i - w_j|}$, and $p = a(e^2 - 1)$. Each branch of the hyperbola is obtained by adding the supplementary condition: $\rho \geq 0$ or $\rho \leq 0$.

From the equation of the hyperbola, it is trivial that any ray from P_i intersects at most once each branch of hyperbola. Therefore, $\mathcal{B}_{ij}$ is star-shaped relatively to P_i, and $\mathcal{V}(P_i)$ is star-shaped relatively to P_i.

The intersection of $\mathcal{B}_{ij}$ and $\mathcal{B}_{ik}$ is the locus of the points M of the plane such as $d(M,P_i) - w_i = d(M,P_j) - w_j = d(M,P_k) - w_k$. This locus corresponds to the centre of the circle externally tangent to the circle's centre P_i radius w_i, centre P_j radius w_j, and centre P_k radius w_k (see thick plain circles on Figure 2). It is a solution of the Apollonius problem (see section 10.11.1 of [Berge79] and Figure 2). It

is also the intersection of $\mathcal{B}_{ij}$ and $\mathcal{B}_{jk}$ and of $\mathcal{B}_{ik}$ and $\mathcal{B}_{jk}$.

According to lemma 3 of [Ash86], $\mathcal{V}(P_i)$ is not empty if, and only if, $|w_i - w_j| < d(P_i, P_j)$.

Ash and Bolker proved that hyperbolic Dirichlet tessellations whose vertices are 3-valent are proper (see Theorem 19 of [Ash86]).

3 THE ALGORITHM

The dual graph of the additively weighted Voronoi diagram is a triangulation. Now, we will examine the events that affect this triangulation.

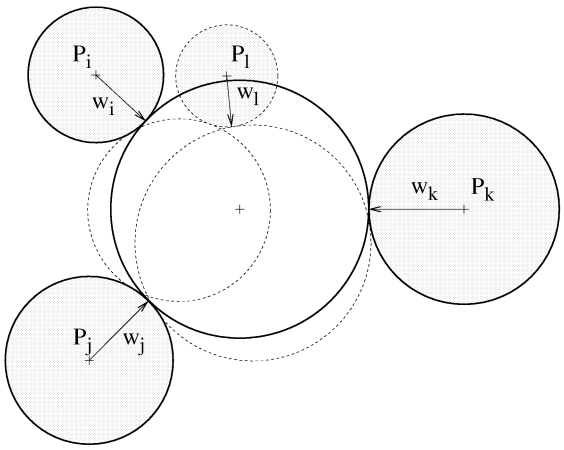

Figure 2: The event that changes the topology

Proposition 1 *(The empty circumcircle criterion for the AW-Voronoi's dual graph): A triangle* $P_i \overset{\triangle}{P_j} P_k$ *exists in the triangulation if, and only if, the circle tangent to the weight circles* $\mathcal{C}(P_i, w_i)$, $\mathcal{C}(P_j, w_j)$, *and* $\mathcal{C}(P_k, w_k)$, *does not intersect any other circle* $\mathcal{C}(P_l, w_l)$, $l \notin \{i, j, k\}$.

Proof. If a fourth circle $\mathcal{C}(P_l, w_l)$ happened to be tangent to the circle $\mathcal{C}_{t_{\{i,j,k\}}}$, that is tangent to $\mathcal{C}(P_i, w_i)$, $\mathcal{C}(P_j, w_j)$, and $\mathcal{C}(P_k, w_k)$, then the vertex $v_{\{i,j,k\}}$ (intersection of $\mathcal{B}_{ij}$, $\mathcal{B}_{ik}$, and $\mathcal{B}_{jk}$) would be 4-valent. This is not possible according to the assumption stated at the beginning of this section. Otherwise, if the intersection of $\mathcal{C}(P_l, w_l)$ and $\mathcal{C}_{t_{\{ijk\}}}$ was constituted by two different points, then $\mathcal{C}_{t_{\{i,j,l\}}}$ and $\mathcal{C}_{t_{\{j,k,l\}}}$ would be tangent to $\mathcal{C}(P_i, w_i)$, $\mathcal{C}(P_j, w_j)$, and $\mathcal{C}(P_l, w_l)$; and $\mathcal{C}(P_j, w_j)$, $\mathcal{C}(P_k, w_k)$, and $\mathcal{C}(P_l, w_l)$ respectively. Then we would have the triangles $P_i \overset{\triangle}{P_j} P_k$, $P_i \overset{\triangle}{P_j} P_l$, and $P_j \overset{\triangle}{P_k} P_l$, which would contradict the fact that the dual graph of the additively weighted Voronoi diagram is a triangulation (see Figure 2). ■

We should therefore make a triangle switch: replace $P_i \overset{\triangle}{P_j} P_k$ and $P_i \overset{\triangle}{P_k} P_l$ by $P_i \overset{\triangle}{P_j} P_l$ and $P_j \overset{\triangle}{P_k} P_l$. Proposition 1 implies that the triangulation mentioned above obeys the Delaunay triangulation "empty circumcircle criterion". This follows the algorithm of Guibas and Stolfi [Guiba85] for the ordinary Voronoi diagram, extending it to this case of a generalized Dirichlet tessellation. This proposition is the basis of the incremental algorithm that we implemented for the dynamic construction and maintenance of additively weighted Voronoi diagrams. When a new point is added, we locate the triangle T in which it lies, then we connect this new point to the triangulation by replacing T by three new triangles whose vertices are the vertices of T and the new point. Then we check every circle tangent to the weight circles of the points of every new triangle. If a triangle switch (see Figure 2) has to be performed (see end of the Proof of Proposition 1), we perform the same check for all the tangent circles corresponding to the triangles generated by the triangle switch (see Figure 2 where the triangle switch is shown: replacing $P_i \overset{\triangle}{P_j} P_k$ and $P_i \overset{\triangle}{P_k} P_l$ by $P_i \overset{\triangle}{P_j} P_l$ and $P_j \overset{\triangle}{P_k} P_l$).

When an existing point is deleted, we locate its nearest neighbour, then we transfer all its neighbours to the nearest neighbour and we remove it and its topological relationships from the triangulation. Then we check every circle tangent to the weight circles of the points of every modified triangle. If a triangle switch has to be performed (see end of the Proof of Proposition 1), we perform the same check for all the tangent circles corresponding to the triangles generated by the triangle switch. This is the basis of the incremental algorithm [Anton98], that we implemented for the dynamic construction and maintenance of additively weighted Voronoi diagrams.

Our algorithm proceeds in a fashion analogous to the algorithm of Devillers, Meiser, and Teillaud [Devil90] for the dynamic Delaunay triangulation based on the Delaunay tree. They proved using the Delaunay tree that each insertion and point location has an expected running time of $O(\log n)$, and each deletion has an expected running time of $O(\log \log n)$. Our algorithm has an efficiency of $O(\log n)$.

3.1 THE JOHNSON-MEHL TESSELLATION

The algorithm for the construction of the dynamic additively weighted Voronoi diagram is the basis of the incremental algorithm we implemented for the construction and maintenance of the Johnson-Mehl model. After each arrival of a new nucleus, the Johnson-Mehl tessellation changes, and we recompute it as follows. The new nucleus is inserted in the Johnson-Mehl tessellation (a new Voronoi region appears), and the neighbouring Voronoi cells are changed. The size of the spheres is then increased by the growth corresponding to the time interval between the previous insertion and this one $(t_i - t_j)$. Consequently, the spheres will be increased for this time interval (see Figures 3 and 4). This type of spatial growth uses a Poisson point process [Okabe92], and we will now introduce two different cases of radial speed for spatial growth processes.

Time homogeneous Poisson point process The uniform radial growth of the nuclei and appearance of their Voronoi regions at two different times is shown in Figures 3 and 4. On Figures 3 and 4, we can see the growth of the spheres between two time units. We notice that the Voronoi regions are changed only when a new particle appears.

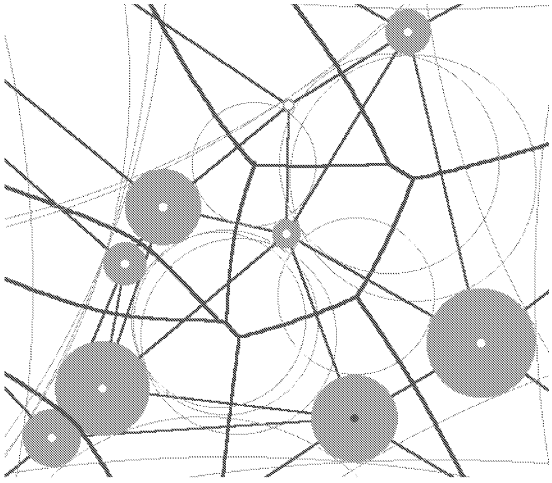

Figure 3: The growth of particles at $t = 93$

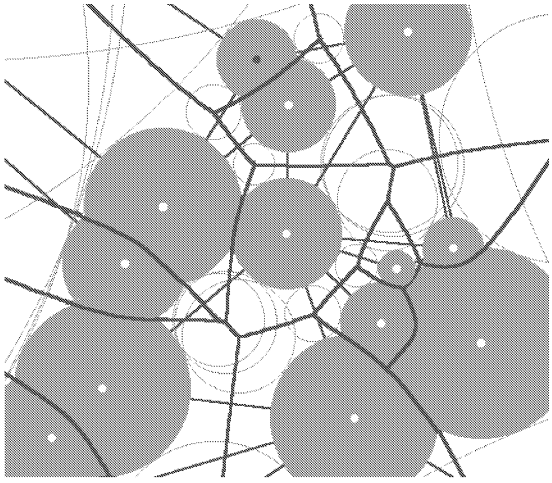

Figure 4: The growth of particles at $t = 163$

We assume [Stoya98] that the radial growth speed is the same for all the spheres, and the growth of the spheres in the portion of contact is stopped (see Figures 3 and 4). In the early stages of growth and nucleations spheres do not overlap, but after a certain time a sphere may touch another sphere [Okabe92].

Time inhomogeneous Poisson point process The Johnson-Mehl model has been generalized [Okabe92] in three different ways: changing the spatial location process for the generators (nuclei), changing the birth rate of the generators, or both. The most extensively studied generalization is the generalization corresponding to the change of the nuclei birth rate as a function of time without changing the spatial location process (the homogeneous Poisson point process). This generalization is known as the time inhomogeneous Johnson-Mehl model. The algorithm for the construction and maintenance of the Johnson-Mehl model is also applied in the case of a time inhomogeneous Poisson point process. In that case, all the nuclei grow at the same radial speed for each time interval and therefore, as long as a new nucleus does not arrive, the difference between the weights of neighbouring nuclei is constant, and the Johnson-Mehl tessellation does not change.

3.2 THE VORONOI GROWTH MODEL

The Additively Voronoi diagram reduces to the ordinary Voronoi diagram when all the w_i are equal to some constant. In that type of particle growth, nucleation occurs simultaneously. In Figure 5 we can see the simultaneous appearance of the nuclei that are all of the same size. Figure 6 shows the growth of these particles after 65 time units (shown in increased weights). We notice that the tessellation has not changed.

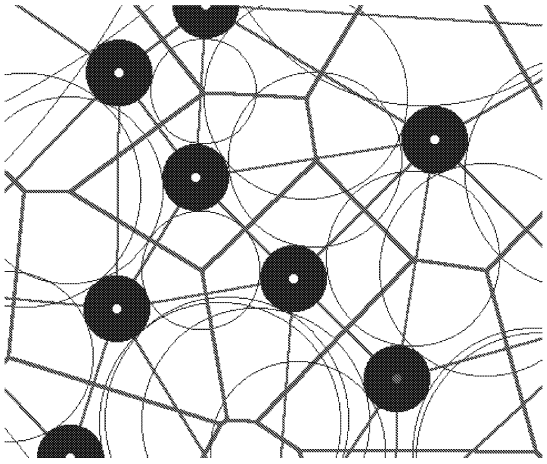

Figure 5: The Voronoi growth model at $t = 31$

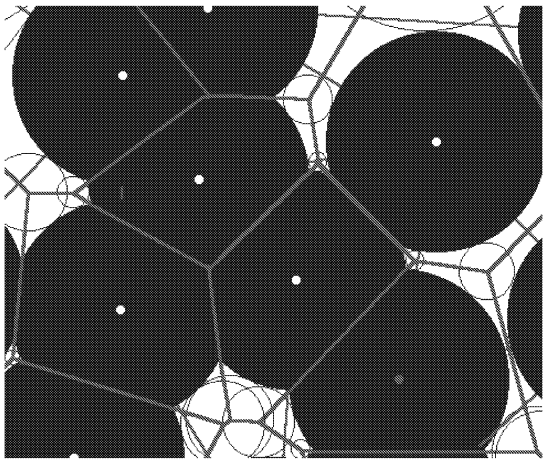

Figure 6: The Voronoi growth model at $t = 96$

Thus, for the nucleation sites that are appearing simultaneously we have a non-Poisson point process [Stoya98] and we can apply our algorithm that reduces the Johnson-Mehl model to the Voronoi growth model.

4 CONCLUSIONS

In this article the algorithm for the visualization of the spatial patterns occurring during the different conditions of nucleation and growth of particles has been presented. Growth models produce spatial patterns as a result of simple growth

processes such as aggregation, agglomeration, and packing [Boots73] and their visualization is important in technological processes. This algorithm is applied in the case of time homogeneous as well as time inhomogeneous Poisson point processes. We use the Poisson point process in the dynamic additively Voronoi diagram to generate the Johnson-Mehl tessellation. The Johnson-Mehl model is a Poisson Voronoi growth model, in which nuclei are generated asynchronously using a Poisson point process, and grow at the same radial speed. Another kind of spatial pattern appears when the nucleation sites appear simultaneously. In that case we have a non-Poisson point process [Stoya98] and we can apply our algorithm that reduces Johnson-Mehl Model to the Voronoi growth model.

These algorithms may be of interest in the visualization of the spatial growth processes investigated in material science and in the determination of physical properties of materials (such as material resistance and deformation). They have many other applications in crystallography, molecular biology and astronomy [Okabe92]. Another potential application lies in the growth of thin films of metal and semiconductors. Finally, these algorithms may be of interest in the application of the Johnson-Mehl tessellations to spatial analysis of retail structures, transportation services and evolution of settlement patterns [Boots73] due to its dynamic nature.

5 ACKNOWLEDGMENTS

The authors have received the financial support from a grants of the Natural Sciences and Engineering Research Council of Canada (NSERC) and the Association des Industries Forestières du Québec (AIFQ).

REFERENCES

[Anton98] Anton, F., Mioc, D., Gold, C.M.: Dynamic Additively Weighted Voronoi Diagrams Made Easy, *Proceedings of the 10th Canadian Conference on Computational Geometry (CCCG'98)*, Montréal, Canada, 1998

[Ash86] Ash, P.F., Bolker, F.D.: Generalized Dirichlet Tessellations, *Geometria Dedicata*, Vol. 20, pp. 209-243, 1986

[Auren88] Aurenhammer, F.: Voronoi diagrams - A survey, *Institute for Information Processing, Technical University of Graz, Report 263*, 1988

[Berge79] Berger, M.: *Géométrie, volume 2 : espaces euclidiens, triangles, cercles et sphères*, CEDIC/FERNAND NATHAN, Paris, 1979

[Boots73] Boots, B.N.: Some models of random subdivision of space, *Geografiska Annaler*, Vol. 55B, pp. 34-48, 1973

[Devil90] Devillers, O., Meiser, S., and Teillaud, M.: Fully Dynamic Delaunay Triangulation in Logarithmic Expected Time per Operation, *Rapport INRIA 1349*, INRIA, BP93, 06902 Sophia-Antipolis cedex, France, 1990

[Guiba85] Guibas, L., and Stolfi, J.: Primitives for the Manipulation of General Subdivisions and the Computation of Voronoi Diagrams, *ACM Transactions on Graphics*, Vol. 4, No. 2, pp. 74-123, 1985

[Horal79] Horalek, V.: The Johnson-Mehl tessellation with time dependent nucleation intensity in view of basic 3-D tessellations, *Mathematical research*, Vol. 51, pp. 111-116, 1979

[Johns39] Johnson, W.A., Mehl, F.R.: Reaction kinetics in processes of nucleation and growth, *Transactions*

of the American Institute of Mining, Metallurgical and Petroleum Engineers, Vol. 135, pp. 416-456, 1939

[Mioc98] Anton, F., Mioc, D., Gold, C.M.: An algorithm for the dynamic construction and maintenance of Additively Weighted Voronoi diagrams, *Proceedings of the 14^{th} European Workshop on Computational Geometry (CG'98)*, Barcelona, Spain, pp. 117-119, 1998

[Okabe92] Okabe, A., Boots, B., Sugihara, K.: *Spatial Tessellations: Concepts and Applications of Voronoi Diagrams*, John Wiley & Sons, 1992

[Stoya98] Stoyan, D.: Random sets: Models and Statistics, *International Statistical Review*, Vol. 66, pp. 1-27, 1998